EurJIC
European Journal of Inorganic Chemistry

Research Article
doi.org/10.1002/ejic.202400511

Chemistry Europe
European Chemical Societies Publishing

www.eurjic.org

Andrographolide Encapsulation in Metal-Organic Frameworks (MOFs) via Solvent-Free Process at High Pressure

Wenndy Pantoja-Romero,[a, b] Yolanda Aysa-Martínez,[c] Alexis Lavín-Flores,[a, b] Nataniel Medina-Berrios,[a, b] Marvin J. Bayro,[a, b] Gerardo Morell,[b, d] Brad R. Weiner,[a, b] and Joaquín Coronas*[c, e]

Andrographolide (ADG) encapsulation was carried out on MOFs MIL-53(Al) and ZIF-8 by high-pressure (0.3 GPa) contact. This methodology is not only environment-friendly but also energy/time-saving and gives rise to ADG-MOFs with physical features equivalent to those of materials obtained by common liquid phase encapsulation. The loaded MOFs were characterized through TEM, SEM, XRD, TGA, FT-IR, BET, and NMR. The observed decrease in the intensity of ADG XRD peaks is due to the adsorption of ADG into the MOFs. TGA showed the decomposition step of ADG in the range of 200–300 °C in both loaded MOFs. FT-IR also showed intense signals of the ADG in the synthesized materials. The dissolution profile of ADG in MIL-53(Al) in PBS (pH = 7.4) was carried out showing that the drug was released up to 96 % after 75 h. Solid-state NMR confirmed the interactions between ADG molecules and ZIF-8 groups and the formation of a hydrogen bond between the carboxylic group of ADG and the hydroxyl group of MIL-53(Al). Coefficient partition studies determined that both MOFs did not improve the hydrophilicity of the ADG, due to the loading of the drug preferably occurring by interactions in the hydrophobic areas within the pores of the MOFs.

Introduction

Metal-organic frameworks (MOFs), also known as porous coordination polymers (PCPs), are a unique class of hybrid solids based on metals and organic ligands that have attracted a lot of attention due to their physical/chemical properties. These compounds are a large class of crystalline materials, with tailorable chemical composition, high porosity, adjustable pore size, and high surface area.[1] These properties are used in a variety of applications including gas storage and separation, heterogeneous catalysis, medical imaging, drug delivery, and light harvesting, among others.[2]

Zeolitic imidazolate frameworks (ZIFs) are a type of MOFs with imidazolates as ligands.[3] In particular, ZIF-8 is stable under physiological conditions (pH 7.4) and is decomposed under acidic conditions.[4] This is crucial for building a drug transport system that is sensitive to pH, as it could not only allow a high capacity of drug loading due to its high porosity but also be pH-activated and release the drug because the Zn–N bond is less stable under acidic conditions. A study reported by Sun et al.[5] showed that the anticancer drug 5-fluorouracil (5-Fu) was loaded into the ZIF-8 nanoparticles, with approximately 50 % of 5-Fu slowly released during the initial stage in a solution of pH 7.4 but the release rate of 5-Fu was significantly increased in a solution of pH 5. Zheng et al.[6] investigated the pH-sensitive drug delivery and anticancer activity using curcumin-loaded ZIF-8 frameworks. Adhikari and colleagues[7] studied the release of doxorubicin in a controlled manner from ZIF-8 and ZIF-7 MOFs by using different triggering agents under external stimuli such as a change in pH. This release was explored in a biomimetic cell membrane.

Carboxylate-based MOF MIL-53(Al) (**M**atériaux de l'**I**nstitut **L**avoisier-Al) is also an excellent candidate as the drug can be delivered due to its three structural forms. The first one is identified as "as-synthesized (as)", which contains within the pores molecules of terephthalic acid because of its synthesis procedure. When the MOF is heated, it undergoes a reversible structural change from a closed pore structure to an open pore structure, labeled as "high temperature (ht)". However, when

[a] W. Pantoja-Romero, A. Lavín-Flores, N. Medina-Berrios, M. J. Bayro, B. R. Weiner
Department of Chemistry, University of Puerto Rico at Rio Piedras Campus, 601 Av. Universidad, San Juan, San Juan, PR

[b] W. Pantoja-Romero, A. Lavín-Flores, N. Medina-Berrios, M. J. Bayro, G. Morell, B. R. Weiner
Molecular Sciences Research Center, University of Puerto Rico at Rio Piedras Campus, 1390 C. Juan, Ponce de León, San Juan 00926, Puerto Rico

[c] Y. Aysa-Martínez, J. Coronas
Instituto de Nanociencia y Materiales de Aragón (INMA), Universidad de Zaragoza-CSIC, Zaragoza 50018, Spain
E-mail: coronas@unizar.es

[d] G. Morell
Department of Physics, University of Puerto Rico at Rio Piedras Campus, 601 Av. Universidad, San Juan, San Juan, PR

[e] J. Coronas
Chemical and Environmental Engineering Department, Universidad de Zaragoza, Zaragoza 50018, Spain

Supporting information for this article is available on the WWW under https://doi.org/10.1002/ejic.202400511

Research Article
doi.org/10.1002/ejic.202400511

the MIL-53(Al) is cooled down, it absorbs water from the environment which induces another structural change: the structure closes, and hence, it is labeled as "low temperature (lt)".[8]

In 2019, Latifi and coworkers[9] synthesized MIL-53(Al) among other MOFs as carriers for thymol (2-isopropyl-5-methylphenol, with antiseptic properties). Thymol was incorporated by a high-pressure method into its host species. The effect of the loaded-MOF was proven in human breast and lung cancer cell lines. Thymol encapsulated MOFs showed more inhibition of cell viability when compared to the non-encapsulated drug.

In traditional liquid phase encapsulation, two methodologies "multi-step" and "one-step" encapsulations are utilized for encapsulating a drug within a MOF.[10,11] The multi-step method involves three sequential steps: synthesizing the MOF, activating it, and then adsorbing the drug in a liquid phase.[12,13] Conversely, the one-step approach incorporates the drug with the reactants during MOF synthesis, enabling the MOF to encapsulate the drug as it forms. Additionally, after encapsulation, reports have indicated the functionalization of MOF particles with various biomolecules and magnetic nanoparticles.[14]

Herein, we encapsulated the drug andrographolide (ADG, a labdane diterpenoid extracted from the stem and leaves of Andrographis paniculata) inside the pores of ZIF-8 and MIL-53(Al). This drug is principally used in the treatment of prostate cancer. ADG has therapeutic potential in humans against liver disorders, cough and cold diseases, infection, inflammation, and. For example, ADG has been shown to inhibit the growth of cancer cells and its 50% growth inhibition ranges from 10–28 μM, depending on the type of cancer cell tested which includes human cancer cell lines.[15] However, this drug has low permeability and solubility, which is a rate-limiting step for drug absorption.[16] For this, the encapsulation of ADG was carried out through a solvent-free process by high-pressure (0.3 GPa) contact in both MOFs as a new method to encapsulate drugs.[17] The solvent-free encapsulation[18] is an environment-friendly alternative to traditional solution-based processes.[19,20] It is intended that high pressure favors the diffusion of the drug into the material porosity and, therefore, the use of any solvent is avoided. The presence of ADG in both MOFs was studied by transmission electron microscope (TEM), scanning electron microscopy (SEM), X-ray diffraction (XRD), thermogravimetric analysis (TGA), Brunauer-Emmett-Teller (BET) analysis, nuclear magnetic resonance (NMR), and Fourier transform infrared (FT-IR) spectroscopy, while their drug release was monitored with a UV-vis spectrophotometer. Finally, to the best of our knowledge, this is the first time that MOFs such as MIL-53(Al) and ZIF-8 (Figure 1a) are applied to encapsulate ADG (Figure 1b) due to their high porosity and chemical and thermal stability.

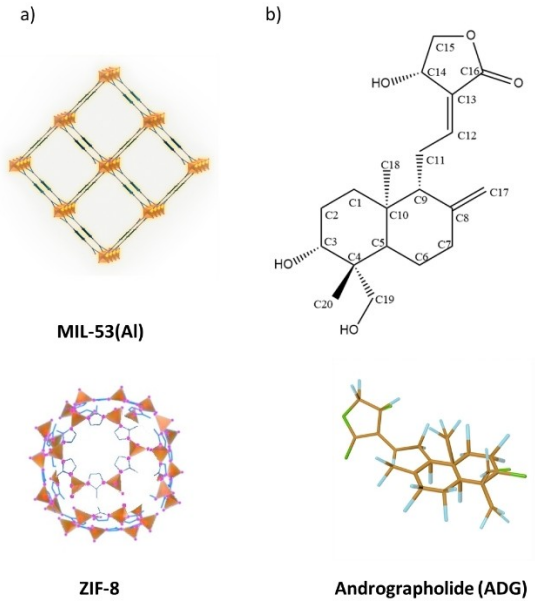

Figure 1. MOF structures (a), and ADG structure (b).

Results and Discussion

Encapsulation of ADG into MOFs

XRD was used to study the encapsulation of ADG. The successful encapsulation of a guest molecule can be monitored with the changes in intensity in the X-ray diffractogram. More specifically, the signals from the guest molecule will decrease upon adsorption in the MOF porosity.[17,20] Diffraction signals for synthesized MIL-53(Al) and ZIF-8 agree with those of both simulated MOFs (Figure S1a and S1b),[8,21] although in case of MIL-53(Al), different peak positions can be observed due to its flexible structure giving rise to the breathing phenomenon.[22]

MIL-53(Al) undergoes a breathing transformation when heated: the solvent is removed from the structure, leaving the pores empty and forming the expanded configuration MIL53(Al)_ht. Upon cooling, water molecules diffuse back (in principle, from the surrounding air) into the pores, closing them through host-guest interactions, resulting in the contracted configuration MIL53(Al)_lt. In this study, given the XRD pattern observed (Figure S1b), MIL-53(Al)_lt was used to load the ADG.[20,22]

The structural transition in flexible MOFs is usually accompanied by enormous changes in the lattice parameters and cell volume as could be noticed for MIL-53(Al).[23] Therefore, Figure 2 shows the comparison of the XRD patterns of the MOFs studied herein (MIL-53(Al), and ZIF-8), ADG and loaded-MOFs at room temperature (ADGZIF8 and ADGMIL53), and 70 °C (ADGMIL53-70 and ADGZIF8-70). ADG was loaded into the MOFs at 70 °C to compare how the temperature affects the process of encapsulation. However, the increase in temperature had no significant change compared to encapsulation at room temperature. Encapsulation of ADG into MIL-53(Al) and ZIF-8 produced a noticeable decrease in the main peak of ADG at 10° (002), as

Research Article
doi.org/10.1002/ejic.202400511

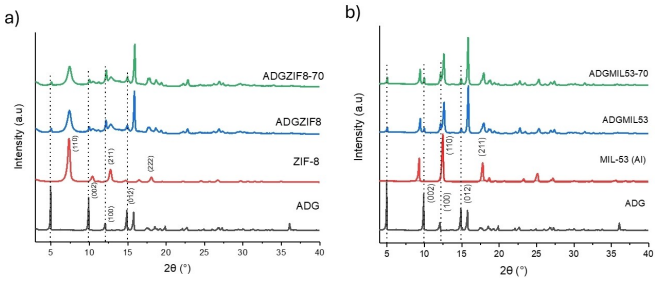

Figure 2. XRD patterns of the different samples (from bottom to top, ADG, MOF, ADG-MOF after high-pressure encapsulation at room temperature and at 70 °C) corresponding to ZIF-8 (a) and MIL-53(Al) (b). 0.3 GPa and 1 : 1 MOF/ADG weight ratio.

inferred from the comparison of the XRD patterns corresponding to the samples of ADGMIL53 and ADGZIF8. Hence, this ADG peak was considered to follow the encapsulation in both MOFs. In addition, all encapsulated materials showed the corresponding peaks of ADG at 11.9° (100) and 15.0° (012),[24] suggesting that some amount of the drug is impregnated outside of the pores of the MOFs. However, it is believed that the decrease in intensity of these peaks is due to the adsorption of ADG into the MOFs. The reduction or absence of the characteristic ADG peaks is consistent with its encapsulation due to the ADG peaks being more evident when the drug is simply mixed with the MOFs by hand mixing in a vial for 1 min without the effect of high pressure (Figure S2). Note that the pressure itself seems to exert an effect on the crystal pattern of ADG promoting the intensity of the ADG peak at ca. 16.0°. This may be caused by crystal modification as a consequence of exposition to high pressure, a phenomenon that is manifested in some drugs, either as new crystal habits, metastable polymorphic forms, or a decrease in the degree of crystallinity.[25,26] Pressure can affect the structure in drugs where molecules are weakly bounded in the crystalline phase by hydrogen bonds and van der Waals forces. In some cases, a phase transition from one polymorphic form to another can occur such as in paracetamol or ibuprofen.[27,28] XRD patterns of ADG powder that were exposed to high pressure (0.3 GPa) were compared with the graphs of powder without being exposed to high pressure (Figure S3). It can be noted that the drug underwent transformations in its crystalline form with slightly wider peaks. Despite this, the encapsulated drug presents characteristic peaks of the drug in which 2·theta values were not modified with pressure (Figure 2).

Nitrogen adsorption and desorption isotherms where obtained for both MOFs (Figure S4a and S4b). The obtained data were applied to calculate the BET specific surface area (SSA) and pore distribution (using the BJH model). Type I isotherms without hysteresis for ZIF-8 and MIL-53(Al) were obtained (with some contribution from adsorption/capillary condensation between MOF particles), which agrees with the fact that these MOFs contain micropores in line with the gas adsorption at low relative pressure. Additionally, nitrogen adsorption was used to probe if the encapsulation was successful in the MOF porosity. A decrease in the BET SSA was observed for ADGMIL53 (2 m^2/g) compared to that of the as-made MIL-53(Al) (1181 ± 23 m^2/g), meaning that the ADG molecules occupied the space inside the porosity of the MOFs as there was less space available for N_2 molecules to adsorb (Figure S5).

Thermal stabilization of ADG after encapsulation, which is related to its adsorption in the MOF porosity (being also evidence of effective encapsulation)[20] was observed through TGA (Figure S6). Figure S6a depicts that ZIF-8 has a small weight loss in the temperature range of 100–400 °C, indicating that the ZIF-8 was stable up to 400 °C. The major weight loss of ZIF-8 takes place in the range of 450–600 °C and can be ascribed to the decomposition of the 2-methylimidazolate ligand. MIL-53(Al) has a loss of adsorbed water (weight loss below 100 °C, something not observed in the hydrophobic ZIF-8) within the pores, while the higher temperature peak is attributed to the decomposition of terephthalate ligand from the MOF framework (Figure S6b). In the TGA curves for ADGZIF8, two removal steps can be observed due to ADG in the range of ca. 200–400 °C and the ZIF-8 in the range of 450–550 °C. The TGA curves for ADGMIL53 and ADGMIL53-70 also show two removal steps due to ADG in the range of 200–350 °C and MIL-53(Al) in the range of 350–550 °C. The TGA curve infections in ADGZIF-8 and ADGMIL53 at ca. 450 °C (Figure S6) allow us to estimate ADG loadings in both MOFs of around 35–40 wt% (ca. 35 wt% for ZIF-8 and ca. 40 wt% for MIL-53(Al), considering roughly the encapsulation step until the inflection point).

FTIR was used to observe the structural changes in the materials obtained and to corroborate the presence of ADG in the samples without losing their chemical integrity. Figure S7a shows that ZIF-8 has a slight peak at 3135 cm^{-1}, which is associated with the aromatic C–H asymmetric stretching vibrations. Another signal around 1635 cm^{-1} corresponds to the C=C stretch mode, while the band at 1585 cm^{-1} is attributed to the C=N stretch vibration. The signals at 1300–1460 cm^{-1} are of the entire ring stretching, whereas the band at 1146 cm^{-1} is derived from aromatic C–N stretching mode. Figure S7b shows the FTIR spectra of MIL-53(Al) which presents the bands at 1608 and 1512 cm^{-1} corresponding to the asymmetric stretching of the –COO group, whereas bands at 1435 and 1417 cm^{-1} corresponding to the symmetric stretching of the –COO group. ADGZIF8, ADGMIL53, ADGZIF8-70, and ADGMIL53-70 show peaks corresponding to the ADG. The peaks at 2800–3000, 1458, and 1220 cm^{-1} are due to the presence of C–H, C=C stretching, and C–O–C of the lactone ring of ADG. However, these samples show displacements in the C=O band of the encapsulated samples concerning pure ADG (1727 cm^{-1}) in Figure S7a and S7b. These vibrations confirm the presence of unchanged ADG molecules (both encapsulated in the MOF microporosity and impregnating it) and are consistent with the interactions between ADG molecules and ZIF-8 C–H groups and the formation of a hydrogen bond between the carboxylic group of MIL-53(Al) and the hydroxyl group of ADG later confirmed in the solid-state NMR.

TEM and SEM were used to study the shape and structure of the MOF particles. The morphology studies of ZIF-8 show a hexagonal shape (Figure 3a), whereas a higher resolution TEM

Research Article
doi.org/10.1002/ejic.202400511

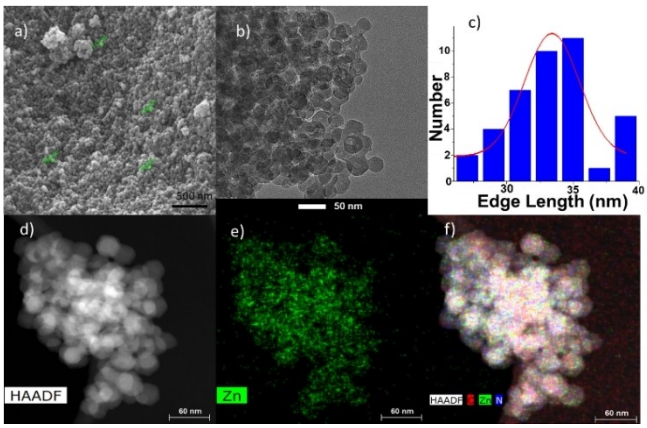

Figure 3. ZIF-8 characterization: a) SEM, b) TEM, c) histogram of sizes, d) HAADF-STEM; EDS mapping e) based on Zn and f) Zn, C, and N.

image is shown in Figure 3c illustrating an average size of 33 nm. High-angle annular dark field scanning transmission electron microscopy (HAADF-STEM) is a technique ideally suited to image metallic nanoparticles in MOF matrices. HAADF-STEM images denote the presence of zinc and nitrogen in ZIF-8 confirmed by the EDS (Figure 3d–f) which match well with what has been observed in the literature.[29] The SEM and TEM images of MIL-53(Al) show ca 1.0 μm×1.6 μm crystals (Figure 4a and b). This size, contrarily to that of ZIF-8 in the nanosize range, suggests that a particle size synthesis study should be done in the future to optimize the application of MIL-53(Al). The presence of aluminum is visible in HAADF-STEM images and confirmed with EDS (Figure 4c and d) as previously reported.[30] Both MOFs show high crystallinity (as demonstrated by XRD characterization) which might be considered appropriate for the encapsulation of ADG at high pressure. Since the MOF crystallinity influences the porosity and in this way the loading of the drug, it is important to have well-defined porous crystalline MOFs to bypass issues related to low drug loading and instability. The hybrids ZIF-8/MIL-53(Al) with ADG show similar particle sizes (Figures S8 and S9).

Solid-state NMR spectroscopy has been widely used to elucidate the structure of various types of solids, due to its sensitivity to the local environment, which is relevant to the study of MOFs.[31] Solid-state ^{13}C magic-angle spinning (MAS) NMR was employed to study the MOF-guest interactions upon encapsulation by high-pressure contact, since this technique is sensitive to changes in the structure upon loading guest molecules. Figure 5 compares the ^{13}C MAS NMR spectra of MIL-53(Al) and ZIF-8 with those MOFs loaded with ADG after encapsulation. Spinning sidebands are seen in all spectra (indicated by asterisks). These are signals that are often attributed to an incomplete averaging by the magic angle spinning process, suggesting that many sites do exhibit a

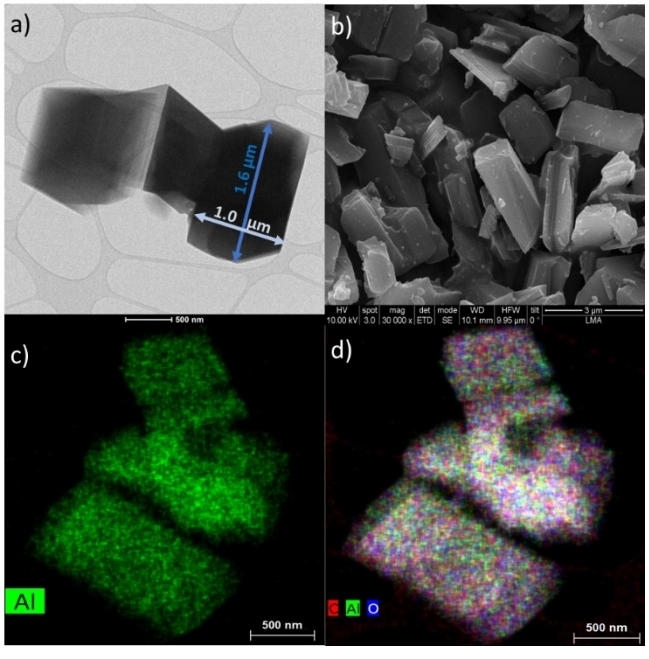

Figure 4. MIL-53 (Al) characterization: a) TEM, b) SEM, c) HAADF-STEM, EDS mapping based on Al, and d) C, Al, and O.

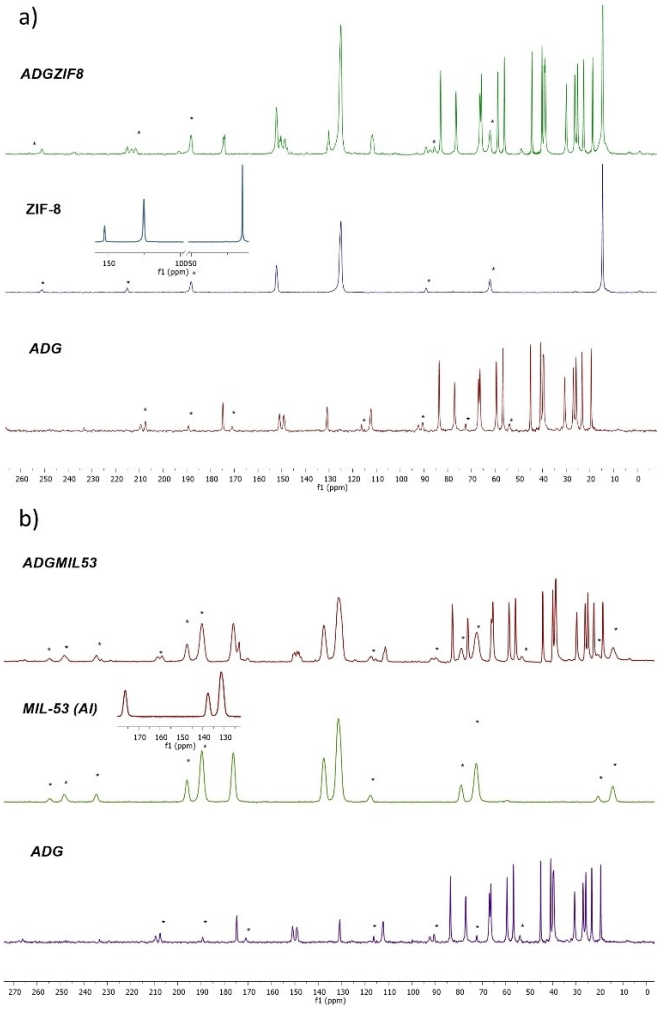

Figure 5. ^{13}C solid-state NMR spectra of the different samples (from bottom to top, ADG, MOF, ADG@MOF after high-pressure encapsulation) corresponding to ZIF-8 a), and MIL-53(Al) (b). Spinning sidebands are indicated by asterisks.

Research Article
doi.org/10.1002/ejic.202400511

significant chemical shift anisotropy (CSA), as would be expected for sp^2 ^{13}C nuclei.[32]

Spectra of the ADGMIL53 complex show that the peaks corresponding to the terephthalate acid of the MOF linker are identical to those in the pristine MIL-53(Al) sample. On the other hand, the signals from ADG are perturbed upon encapsulation. While relative peak positions are mostly unchanged, there is evident line broadening of the ADG signals, both in downfield and upfield positions. In general, line broadening can be attributed to a disruption in the crystalline order due to the interpenetration of both host and guest materials. The additional line broadening observed in downfield ADG signals in the complex is likely due to the aromatic ring effect in the linker, which induces a magnetic field that affects the anisotropy and deshielding of carbonyl groups. Therefore, the size and shape of ADG and MIL-53(Al) determine the symmetric position in which the drug penetrates into the cavity of the MOF.

In the case of ZIF-8, a peak at 14 ppm is observed for the methyl group, while the two resonances at 124 and 152 ppm correspond to the two aromatic nuclei in the linker and indicate that the diamagnetic Zn metal center forms a uniform assembly with the linker. An outstanding characteristic of the ZIF-8 is that it has a methyl group, which introduces greater heterogeneity and produces a narrow signal due to efficient self-decoupling driven by rapid methyl hopping motion. ADGZIF8 has several signals with lower intensity compared to pristine ADG, but the line broadening in the drug is less pronounced than in ADGMIL-53. However, the hydroxyl-linked carbon in the five-membered ring (at 66 ppm) of ADG shows significant line broadening in the ZIF8 complex, indicating possible intermolecular interactions such as hydrogen bonding. There is also a slight shift in the $-CH_3$ signal of the MOF, which may occur because methyl groups are more susceptible to symmetry changes when in contact with other molecules. Therefore, the methyl group and the hydrogen atoms corresponding to the carbon-carbon double bonds of 2-methylimidazole in ZIF-8 appear to constitute the preferred adsorption sites for ADG encapsulated molecules. On the other hand, the symmetry of the MOF linker is not affected and the ^{13}C NMR peaks are similar to those of the pristine MIL-53(Al) and ZIF-8.

Release of ADG Inside of Pores of the MOFs

To investigate the possibility of using the synthesized loaded-MOFs as drug carriers, the release of ADG was examined by UV-Vis spectroscopy using PBS as biological media simulating a pH = 7.4. The experiments were only carried out with MIL-53(Al) since ZIF-8 has an absorption peak in the same region as the drug (220 nm), which makes it non-trivial to study with this technique (Figure S10). For this reason, a calibration curve was constructed from a series of standard solutions (Figure S11a). The absorbance increased as the concentration increased, as explained in Beer-Lambert's law. Figure S11b shows the obtained calibration curve with an $R^2 = 0.99996$. The experiments were carried out in triplicate.

The experiments were carried out for a maximum of 75 h under biological conditions (Figure 6). The ADG release from MIL-53(Al) shows that the process was faster in the first 25 h, whereas in the following 25–75 h, the process became slower. The reason for which the release is faster in the first hours is due to the drug that is impregnated outside of the MOF, followed by the drug that is encapsulated inside the micropores of the MOF. Additionally, the percentage of ADG released after 75 h was calculated to be 96(±1.2)%. These results show that, after the progressive first release, an important partof the initial ADG is released (about 20%) at 37 °C after 30 h suggesting a strong ADG-MOF affinity. This is likely due to the large porosity (windows, cages) and flexibility[17,33] of the MOFs that facilitated the diffusion of the ADG. Finally, the mass balance carried out after finalizing the release experiment (determining the drug in the solution after the long term release) allowed to determine a ca. 37 wt.% loading of ADG in MIL-53(Al), in good agreement with the previous ca. 40 wt.% estimated by TGA.

Partition Coefficient Studies

Hydrophobic/hydrophilic balance is a key parameter since MOFs possess both a polar fraction (metal clusters) and a nonpolar one (ligands). The value of the Log P is represented as hydrophilicity (in a range between 0 and 2), hydrophobicity (in a range between 0 and 2), and amphiphilic (0) character for each compound.

Log P results obtained using D_2O at a neutral pH as the aqueous phase showed that both MIL-53(Al) and ZIF-8 did not improve the hydrophilicity of the ADG (Figure 7). Instead, a slight increase in hydrophobicity was observed when the drug was encapsulated within MIL-53(Al) and ZIF-8. The hydrophobicity of MOFs is characterized by their contact angles (CAs) with water. MOFs with CAs below 90° are considered hydrophilic, between 90° and 150° are referred to as hydrophobic, and those with CAs greater than 150° are termed as superhydrophobic.[34,35] ZIF-8 exhibits a strong hydrophobicity with a water contact angle of 142°[36] while MIL-53(Al) is a slightly hydrophilic MOF since it has a free –OH linked to

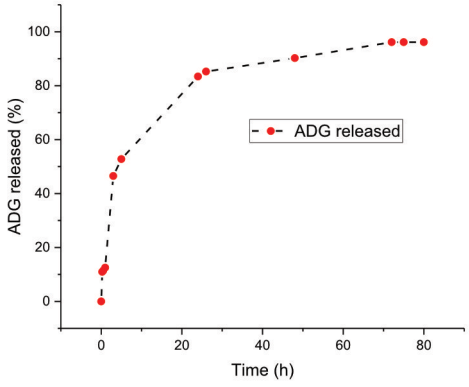

Figure 6. ADG released from MIL-53(Al) at 37 °C.

Research Article
doi.org/10.1002/ejic.202400511

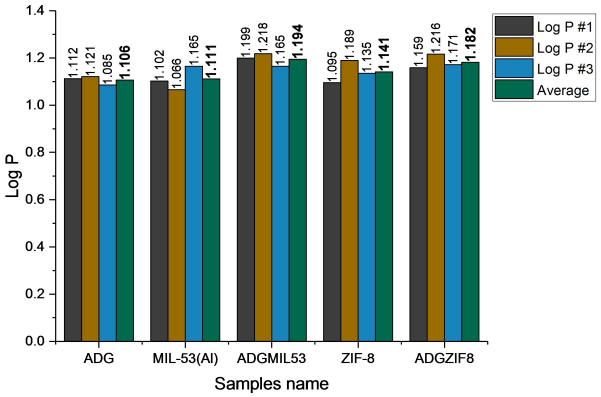

Figure 7. Histograms for Log P tests by NMR method for MOFs and loaded-MOFs compared to ADG.

aluminum and a contact angle of 86°,[37] which can be seen in the log P results shown in Figure 7. Despite this, when ADG is encapsulated in MIL-53(Al), its hydrophobicity (log P = 1.182) is slightly higher than that of ADG encapsulated in ZIF-8 (log P = 1.194). This could be because of a greater amount of encapsulated ADG in the pores of the MIL-53(Al) as can be noted in the TGA results (Figure S6b). However, when talking about CA, the sample roughness derived from the different particle sizes can affect the measurement.

The drug was loaded within the MIL-53(Al) in its hydrophobic areas, as shown by the disappearance of the ^{1}H NMR peaks at 7.41 ppm, and 7.27 ppm, corresponding to the protons in the terephthalate benzene ring (Figure S12). ADG is associated via its terminal double bond, as can be noted by the disappearance of the signal of its proton in C12 position (Figure 1b) at 6.62 ppm shown in Figure S13. In the case of the ZIF-8 (Figure S14), the drug is associated with the side of the imidazole's carbon-carbon double bond, as seen by the shift of the double bond proton at 7.08 ppm. This association occurred mainly via the drug terminal alkene since its signal at 7.38 ppm disappeared (Figure S15). Both with MIL-53(Al) and ZIF-8, the loading of the drug was driven by interactions in the hydrophobic areas within the pores of the MOFs. Finally, the ADG-MOF encapsulation strategy shown in this work might allow for a reduction in the dose required for conventional chemotherapy, increasing in turn its therapeutic efficacy, and thus diminishing undesired side effects, despite that ADG did not improve its hydrophilicity upon encapsulation.

Conclusions

ZIF-8 and MIL-53(Al) were synthesized successfully and were used to load the drug ADG inside their pores. An encapsulation was carried out using a solvent-free method by a high-pressure process. The XRD patterns, N_2 adsorption isotherms, FT-IR, NMR spectra, and TGA curves demonstrated the successful encapsulation of the drug. The combination of the characterization techniques demonstrated that the ADG was inside the pores of the MOFs, due to the signal characteristics of the drug being relevant in each one of the analyses carried out. However, some amount of the drug is impregnated outside of the pores of the MOFs, in agreement with a UV-vis using PBS release (physiological conditions pH 7.4) in two stages, in the case of MIL-53(Al): one faster for the impregnated ADG and the other slower for the properly encapsulated in the microporosity of the MOF. Hence, pH activated release under acidic conditions could be studied in the future. Finally, the outcomes achieved in this work, obtained through a green process, allow the encapsulation process to be simpler, and although the solubility (in terms of the hydrophobicity changes revealed by ^{1}H NMR) of the drug did not improve it would help in its potential as an anti-cancer drug.

Experimental Section

Synthesis of MIL-53(Al)

Following a previous report for the synthesis of MIL-53(Al),[4] 5.2 g (13.9 mmol) of aluminum nitrate nonahydrate (Sigma Aldrich, 98%) and 1.12 g (6.7 mmol) of terephthalic acid (Sigma Aldrich, 98%) were dissolved in 20 mL of distilled water and placed in a Teflon-lined steel autoclave for 3 days at 220 °C. The product was recovered by centrifugation at 10,000 rpm for 10 min, washed once with ethanol by centrifugation under the same conditions, and dried overnight at 65 °C. The solid was activated by calcination at 380 °C for 24 h.

Synthesis of ZIF-8

To obtain ZIF-8,[14] two different solutions were prepared. First, 2.93 g (9.87 mmol) of zinc nitrate hexahydrate (Sigma Aldrich, 98%) was dissolved in 200 mL of methanol in a spherical flask. Secondly, 6.489 g of 2-methylimidazole (79.04 mmol) in 200 mL of MeOH was prepared in parallel. The former solution was then added to the latter and stirred at room temperature for 30 min. The product was centrifugated at 8,000 rpm for 15 mins and washed twice with 50 mL of fresh MeOH. The final product was then dried overnight at either room temperature or 70 °C.

Encapsulation of ADG in MIL-53(Al) and ZIF-8

ADG was encapsulated following the solvent-free encapsulation process,[13] which is considered environmentally friendly, in comparison with others, by avoiding the use of solvents entirely. The procedure consists of high-pressure encapsulation. First, 75 mg of MOF (ZIF-8 and MIL-53(Al)) and 75 mg of ADG (weight ratio 1:1) are thoroughly mixed, by shaking the mixture by hand in a vial for 1 min. The mixture is placed at room temperature or 70 °C for both MOFs inside a metal cylinder of a hydraulic press. With a metal piston, the solids are then compacted under 0.3 GPa of pressure for 15 min.

Andrographolide Release

Calibration Curve

A stock solution of 0.5 mg/mL of ADG in phosphate-buffered saline (PBS) was prepared. Then, 2-fold serial dilutions were performed to obtain eight standard solutions in concentrations of 0.3, 0.2, 0.1, 0.08, 0.05, 0.03, and 0.01 mg/mL. Absorbance was measured using

a V-670 Jasco UV-vis spectrophotometer (200–500 nm) and PBS was employed as a solvent blank. The wavelength of maximum absorbance (λ(max)) for ADG was identified at 220 nm.

Release Experiment

In a 250 mL beaker, 100 mL of PBS was transferred and left under constant stirring at 150 rpm and 37 °C. An aliquot of 1 mL was taken before the addition of the loaded-MOF to record the first time point (0 h). Subsequently, 15 mg of ADG-MIL53(Al) was added to the buffer. Aliquots (1 mL) were collected after each selected time point (0.25, 0.5, 1, 3, 5, 24, 48, and 72 h) and diluted with PBS in a 25 mL volumetric flask. The absorbance of ADG released from the MIL-53(Al) was measured at 222 nm. The experiment was performed in triplicate.

Acknowledgements

This research was carried out under the auspices of the Fundación Carolina España, PR NASA EPSCoR (NASA Cooperative Agreement [NNX15AK43A]) and the Research Initiative for Scientific Enhancement program (RISE [5R25GM061151-20]). We want to acknowledge Mr. Kim Kisslinger from Brookhaven National Institute -New York for taking HR-TEM images. To Mr. Guillermo Blazquez García, for his contributions in Figure 1, image creation and editing. is gratefully acknowledged. We also acknowledge funding in part from the National Institutes of Health/National Cancer Institute under Grant #U54 CA096297, grant PID2022-138582OB-I00 funded from the Spanish Agencia Estatal de Investigación and Ministerio de Ciencia e Innovación and by "ERDF a way of making Europe" and grant T68-23R from the Aragón Government.

Conflict of Interests

The authors declare no conflict of interest.

Data Availability Statement

The data that support the findings of this study are available from the corresponding author upon reasonable request.

Keywords: Metal-organic frameworks · Organic-inorganic hybrid composites · High-pressure chemistry

[1] H. Wang, Q. Zhu, R. Zou, Q. Xu, *CHEM* **2017**, *2*(1), 52–80, DOI: 10.1021/acsenergylett.9b02625.
[2] Y. R. Lee, M. S. Jang, H. Y. Cho, H. J. Kwon, S. Kim, W. S. Ahn, *Chem. Eng. J.* **2015**, *271*, 276–280, DOI: 10.1016/j.cej.2015.02.094.
[3] K. S. Park, Z. Ni, A. P. Cote, J. Y. Choi, R. Huang, F. J. Uribe-Romo, H. K. Chae, M. O'Keeffe, O. M. Yaghi, *Proc. Natl. Acad. Sci.* **2006**, *103*(27), DOI: 10.1073/pnas.0602439103.
[4] M. D. J. Velásquez-Hernández, R. Ricco, F. Carraro, F. T. Limpoco, M. Linares-Moreau, E. Leitner, H. Wiltsche, J. Rattenberger, H. Schröttner, P. Frühwirt, E. M. Stadler, G. Gescheidt, H. Amenitsch, C. J. Doonan, P. Falcaro, *Cryst. Eng. Comm.* **2019**, *21*(31), 4538–4544, DOI: 10.1039/C9CE00757A.
[5] C. Y. Sun, C. Qin, X. L. Wang, G. S. Yang, K. Z. Shao, Y. Q. Lan, Z. M. Su, P. Huang, C. G. Wang, E. B. Wang, *Dalt. Trans.* **2012**, *41*(23), 6906–6909, DOI: 10.1039/c2dt30357d.
[6] M. Zheng, S. Liu, X. Guan, Z. Xie, *ACS Appl. Mater. Interfaces* **2015**, *7*(40), 22181–22187, DOI: 10.1039/c2dt30357d.
[7] C. Adhikari, A. Das, A. Chakraborty, *Mol. Pharm.* **2015**, *12*(9), 3158–3166, DOI: 10.1021/acs.molpharmaceut.5b00043.
[8] T. Loiseau, C. Serre, C. Huguenard, G. Fink, F. Taulelle, M. Henry, T. Bataille, G. Férey, *Chem. - A Eur. J.* **2004**, *10*(6), 1373–1382, DOI: 10.1002/chem.200305413.
[9] L. Latifi, S. Sohrabnezhad, *Polyhedron* **2020**, *180*, 114321, DOI: 10.1016/j.poly.2019.114321.
[10] L. Paseta, G. Potier, S. Abbott, J. Coronas, *Org. Biomol. Chem.* **2015**, *13*(6), 1724–1731, DOI: 10.1039/c4ob01898b.
[11] A. T. Sose, H. D. Cornell, B. J. Gibbons, A. A. Burris, A. J. Morris, S. A. Deshmukh, *RSC Adv.* **2021**, *11*(28), 17064–17071, DOI: 10.1039/d1ra01746b.
[12] Z. L. Mensinger, B. L. Cook, E. L. Wilson, *ACS Omega* **2020**, *5*(51), 32969–32974, DOI: 10.1021/acsomega.0c04019.
[13] R. Anand, F. Borghi, F. Manoli, I. Manet, V. Agostoni, P. Reschiglian, R. Gref, S. Monti, *J. Phys. Chem. B* **2014**, *118*(29), 8532–8539, DOI: 10.1021/jp503809w.
[14] J. Zhuang, C. H. Kuo, L. Y. Chou, D. Y. Liu, E. Weerapana, C. K. Tsung, *ACS Nano* **2014**, *8*(3), 2812–2819, DOI: 10.1021/nn406590q.
[15] R. Ajaya Kumar, K. Sridevi, N. Vijaya Kumar, S. Nanduri, S. Rajagopal, *J. Ethnopharmacol.* **2004**, *92*(2–3), 291–295, DOI: 10.1016/j.jep.2004.03.004.
[16] S. Y. K. Fong, M. Liu, H. Wei, R. Löbenberg, I. Kanfer, V. H. L. Lee, G. L. Amidon, Z. Zuo, *Mol. Pharm.* **2013**, *10*(5), 1623–1643, DOI: 10.1021/mp300502m.
[17] R. Monteagudo-Olivan, L. Paseta, G. Potier, P. López-Ram-de-Viu, J. Coronas, *Eur. J. Inorg. Chem.* **2019**, *2019*(1), 29–36, DOI: 10.1002/ejic.201800985.
[18] M. García-Palacín, J. I. Martínez, L. Paseta, A. Deacon, T. Johnson, M. Malankowska, C. Téllez, J. Coronas, *ACS Sustain. Chem. Eng.* **2020**, *8*(7), 2973–2980, DOI: 10.1021/acssuschemeng.9b07593.
[19] H. Cumming, C. Rücker, *ACS Omega* **2017**, *2*(9), 6244–6249, DOI: 10.1021/acsomega.7b01102.
[20] B. Zornoza, C. Rubio, E. Piera, M. A. Caballero, D. Julve, J. Pérez, C. Téllez, J. Coronas, *ACS Appl. Mater. Interfaces* **2022**, *14*, 22476–22488, DOI: 10.1021/acsami.2c04293.
[21] M. Adnan, K. Li, L. Xu, Y. Yan, *Catalysts* **2018**, *8*(3), 1–14, DOI: 10.3390/catal8030096.
[22] P. Serra-Crespo, A. Dikhtiarenko, E. Stavitski, J. Juan-Alcañiz, F. Kapteijn, F. X. Coudert, J. Gascon, *CrystEngComm* **2015**, *17*(2), 276–280, DOI: 10.1039/c4ce00436a.
[23] A. Schneemann, V. Bon, I. Schwedler, I. Senkovska, S. Kaskel, R. A. Fischer, *Chem. Soc. Rev.* **2014**, *43*(16), 6062–6096, DOI: 10.1039/c4cs00101j.
[24] C. C. Yen, Y. K. Liang, C. P. Cheng, M. C. Hsu, Y. T. Wu, *Int. J. Mol. Sci.* **2020**, *21*(7), DOI: 10.3390/ijms21072506.
[25] B. Ibraheem, K. G. Wagner, *Int. J. Pharm. X* **2021**, *3(March)*, 100075, DOI: 10.1016/j.ijpx.2021.100075.
[26] D. Braga, L. Casali, F. Grepioni, *Int. J. Mol. Sci.* **2022**, *23*(16), DOI: 10.3390/ijms23169013.
[27] A. Nokhodchi, O. Amire, M. Jelvehgari, *Daru* **2010**, *18*(2), 74–83.
[28] E. V. Boldyreva, *J. Mol. Struct.* **2004**, *700*(1–3), 151–155, DOI: 10.1016/j.molstruc.2004.03.026.
[29] O. Kolmykov, J. M. Commenge, H. Alem, E. Girot, K. Mozet, G. Medjahdi, R. Schneider, *Mater. Des.* **2017**, *122*, 31–41, DOI: 10.1016/j.matdes.2017.03.002.
[30] D. V. Patil, P. B. S. Rallapalli, G. P. Dangi, R. J. Tayade, R. S. Somani, H. C. Bajaj, *Ind. Eng. Chem. Res.* **2011**, *50*(18), 10516–10524, DOI: 10.1021/ie200429f.
[31] R. Giovine, C. Volkringer, J. Trébosc, J. P. Amoureux, T. Loiseau, O. Lafon, F. Pourpoint, *Sect. C Struct. Chem.* **2017**, *73*(3), 176–183, DOI: 10.1107/S2053229616017915.
[32] S. Sneddon, J. Kahr, A. F. Orsi, D. J. Price, D. M. Dawson, P. A. Wright, S. E. Ashbrook, *Solid State Nucl. Magn. Reson.* **2017**, *87(August)*, 54–64, DOI: 10.1016/j.ssnmr.2017.09.001.
[33] N. Liédana, A. Galve, C. Rubio, C. Téllez, J. Coronas, *ACS Appl. Mater. Interfaces* **2012**, *4*(9), 5016–5021, DOI: 10.1021/am301365h.
[34] L. H. Xie, M. M. Xu, X. M. Liu, M. J. Zhao, J. R. Li, *Adv. Sci.* **2020**, *7*(4), DOI: 10.1002/advs.201901758.
[35] S. Mukherjee, S. Sharma, S. K. Ghosh, *APL Mater.* **2019**, *7*(5), DOI: 10.1063/1.5091783.

Research Article
doi.org/10.1002/ejic.202400511

[36] E. E. Sann, Y. Pan, Z. Gao, S. Zhan, F. Xia, *Sep. Purif. Technol.* **2018**, *206*, 186–191, DOI: 10.1016/j.seppur.2018.04.027.
[37] L. Zhu, H. Yu, H. Zhang, J. Shen, L. Xue, C. Gao, B. Van Der Bruggen, *RSC Adv.* **2015**, *5*(89), 73068–73076, DOI: 10.1039/c5ra10259f.

Manuscript received: August 6, 2024
Accepted manuscript online: October 21, 2024
Version of record online: November 13, 2024